Clays and Clay Minerals, Vol. 46, No. 2, 183–194, 1998.

RAPID, ACCURATE PHASE QUANTIFICATION OF CLAY-BEARING SAMPLES USING A POSITION-SENSITIVE X-RAY DETECTOR

MERYL BATCHELDER AND GORDON CRESSEY

Department of Mineralogy, The Natural History Museum, Cromwell Road, London, SW7 5BD, UK

Abstract—The rapid phase quantification method using X-ray diffraction (XRD) with a position-sensitive detector (PSD), outlined by Cressey and Schofield (1996), has been extended to facilitate mineral phase quantification of clay-bearing samples. In addition, correction factors for differences in matrix absorption effects have been calculated and applied. The method now enables mudrock mineralogy to be quantified rapidly and efficiently. Using this approach overcomes many of the problems hitherto associated with the quantitative analysis of clay minerals, in particular the effects of preferred orientation of crystallites and variable sample-area irradiation, that make the task of quantification extremely difficult by conventional Bragg–Brentano scanning diffractometry.

Key Words—Absorption Correction, Mudrocks, Position-sensitive Detector, Quantification, X-ray Diffraction.

INTRODUCTION

Quantitative analysis of phase proportions by XRD using internal and external standards (Chung 1974a, 1974b) and employing whole-pattern methods (Smith et al. 1987) and Rietveld methods (Hill and Howard 1987; Bish and Howard 1988) are well documented. The quantitative analysis of clay mineral proportions in mixed-assemblage samples has been reviewed by Brindley (1980), Moore and Reynolds (1989), McManus (1991) and Snyder and Bish (1989).

Many procedures for quantitative analysis rely upon internal standards, laborious sample preparation and tedious data processing. Peak interference and the suitability of the standard constitute 2 major obstacles in quantitative analysis. The state of disaggregation, alteration from chemical pretreatment, particle size separation, preferred orientation of crystallites in the prepared sample and the method of assessing clay mineral proportions from the diffraction pattern may all contribute to errors in quantification (McManus 1991). Published methods of quantitative analysis for clay-bearing samples commonly result in standard deviations of up to 20% (Moore and Reynolds 1989).

Foster and Wolfel (1988) utilized an early, curved PSD system in transmission mode for quantitative analysis. Although the method was rapid, their accuracy was limited, errors being generated from sample loading and transmission absorption measurements. In the present study, we have acquired XRD data using a curved PSD. Our experiments are in reflection rather than transmission mode, and we calculate matrix absorption correction factors. We employ conventional whole-pattern fitting to analyze these data, and demonstrate that the PSD-XRD method is a rapid and accurate technique that avoids many of the pitfalls hitherto associated with the quantification of clay-bearing samples by XRD.

EXPERIMENTAL

Our quantification method utilizes a curved PSD with an output array consisting of 4096 channels representing an arc of 120 °2θ (0.03° channel width). This detector enables diffraction patterns to be acquired rapidly by measuring diffracted intensity at all angles simultaneously around the 120° arc. The use of an anode blade rather than a fragile anode wire within a new generation of such detectors allows reliable, high-precision, high-quality diffraction patterns to be recorded extremely rapidly. The resolution of the PSD is sufficiently good to record all the subtle details in the inherently broad peak patterns from clays. Our data were collected using an Enraf-Nonius PDS 120 (Powder Diffraction System 120) with a curved PSD and a fixed beam-sample-detector geometry. A germanium 111 monochromator was used to select only Cu$K\alpha_1$ radiation from the primary beam and tube operating conditions were 45 kV and 45 mA. Horizontal and vertical slits between the monochromator and sample were used to restrict the beam to 0.24 × 5.0 mm, respectively, and thus, the irradiated area was constant for each experiment. Measurements were made in reflection geometry with the powder sample surface at a fixed angle of ~5° to the incident beam. The sample was rotated continuously in its own plane which statistically increases the number of crystallites orientated in diffracting positions (Brindley 1980). The tilt of the sample surface to the beam was held constant during data acquisition, but can be altered by a micrometer adjustment control. This angle can be reproduced with high precision for subsequent experiments. If desired, the incidence angle can be chosen to avoid the Bragg angle of a crystallite set lying in

preferred orientation. Data acquisition times of only 10 min were used for the majority of the analyses. NIST silicon powder (SRM 640) was used (unground) as an external standard for the 2θ calibration. The 2θ linearization was performed with the ENRAF-GUFI software using a least-squares cubic spline function. All mineral standards used in this study are from the mineral collection at the Natural History Museum, London, United Kingdom.

Theoretical Considerations

The diffracted intensity from *hkl* planes in a single-phase flat powder sample can be expressed as:

$$I^{A}_{hkl} = t\left(\frac{I_o k m \mathrm{Lp}}{\mu^{A}}\right) F^{2}_{hkl} V^{A} \qquad [1]$$

where t is the detector counting time, I_o is the direct beam intensity, k is an experimental constant, m is the multiplicity of reflection *hkl*, Lp is the Lorenz-polarization factor, μ^A is the linear absorption coefficient for phase A and V^A is the volume of diffracting crystals. For phase A in a mixed-assemblage sample, the diffracted intensity will be reduced relative to that recorded under identical conditions from a sample containing 100% A and the ratio of diffracted intensities will be given by:

$$\frac{I^{A'}_{hkl}}{I^{A}_{hkl}} = \left(\frac{\mu^{A}}{\mu'}\right)\frac{\nu^{A}}{V^{A}} \qquad [2]$$

where $I^{A'}_{hkl}$ is the diffracted intensity for phase A in the mixture, μ' is the linear absorption coefficient of the total matrix and ν^A is the volume fraction of phase A in the mixture. The diffracted intensity from phase A in a sample diluted by other phases will be reduced in direct proportion to the volume fraction of phase A in the mixture. The intensity observed is also a function of absorption by the sample, the incident beam flux and the total counting time by the detector. The whole diffraction pattern (including sharp and diffuse scattering characteristics) from component A in the mixture will be proportionally reduced in intensity relative to the standard pattern (100% A). Any part(s) of the diffraction signature can be used to assess the phase proportions. Taking I^{A}_{hkl} and V^{A}_{hkl} of the standard as unity, the quantification procedure using whole-pattern assessment can be summarized thus:

$$X^{A} = \left(\frac{t'}{t}\right)\left(\frac{I_o'}{I_o}\right)\left(\frac{\mu^{A}}{\mu'}\right)\nu^{A} \qquad [3]$$

where X^A is the pattern intensity fraction relative to the standard (pure A) and t and t' are the acquisition times of the standard and mixed-assemblage patterns respectively. I_o and I_o' represent the incident beam flux during acquisition of standard and mixed-assemblage patterns, respectively. This relationship can be used quantitatively, provided that a constant sample volume is irradiated by the X-ray beam. For phases with similar linear absorption coefficients we can easily demonstrate that application of Equation [3] yields accurate quantification of phases in known mixtures. The reproducibility of the results indicates that similar packing densities are achieved and therefore the sample volume irradiated is almost constant. In cases where matrix absorption does affect penetration depth, a correction can be applied after pattern stripping; this aspect is discussed later. Using a PSD system and reproducible sample volume conditions, the diffracted intensity is also proportional to pattern acquisition time. Standard patterns need not necessarily be acquired over a counting-time period equivalent to that of any multiphase sample, as patterns to be compared can be proportioned appropriately during data analysis. Any differences in incident beam X-ray flux can be taken into account using the method described by Cressey and Schofield (1996) where the backgrounds of the external Si calibrant patterns associated with each experimental session are used as a relative measure of total X-ray flux at the sample.

Sample Preparation

Although not a standard technique, we employ a simple sample preparation method for all our experiments. Samples were only gently ground until a smooth powder was produced. The whole sample was then sieved to less than 37 μm to reduce extreme particle-size gradients and avoid segregation. Separation, glycolation or heating of the clay-sized fraction is not necessary for phase quantification by our method. Dry samples were top loaded into a circular well mount, 15 mm in diameter and 1 mm deep. To avoid inducing a high degree of preferred orientation of platy crystals parallel to the top surface, each sample was packed and levelled using only the narrow (knife) edge of a small steel spatula until a smooth flat surface was obtained that was level with the rim of the circular well holder. The packing procedure took less than 1 min per sample. Figure 1 demonstrates the very high degree of pattern reproducibility obtained using this easy method of sample preparation for a smectite (BM 32737), repeatedly removed and repacked in a deep well mount 5 times, shown in diffraction patterns b) to f). For comparison, diffraction pattern a) is the result obtained by deliberately flattening the surface of the powder with the flat face of the spatula; this produced considerable preferred orientation and enhanced the 001 peak intensity at 5.7 °2θ, because the angle of incidence of the beam with the sample surface is close to the Bragg angle for the 001 reflection. However the effect of this preferred orientation on the rest of the pattern is minimal and the 2-dimensional scattering at higher angles of 2θ is almost identical to that of the non-oriented samples. Even with a degree of preferred orientation present, apart from the single 001 reflec-

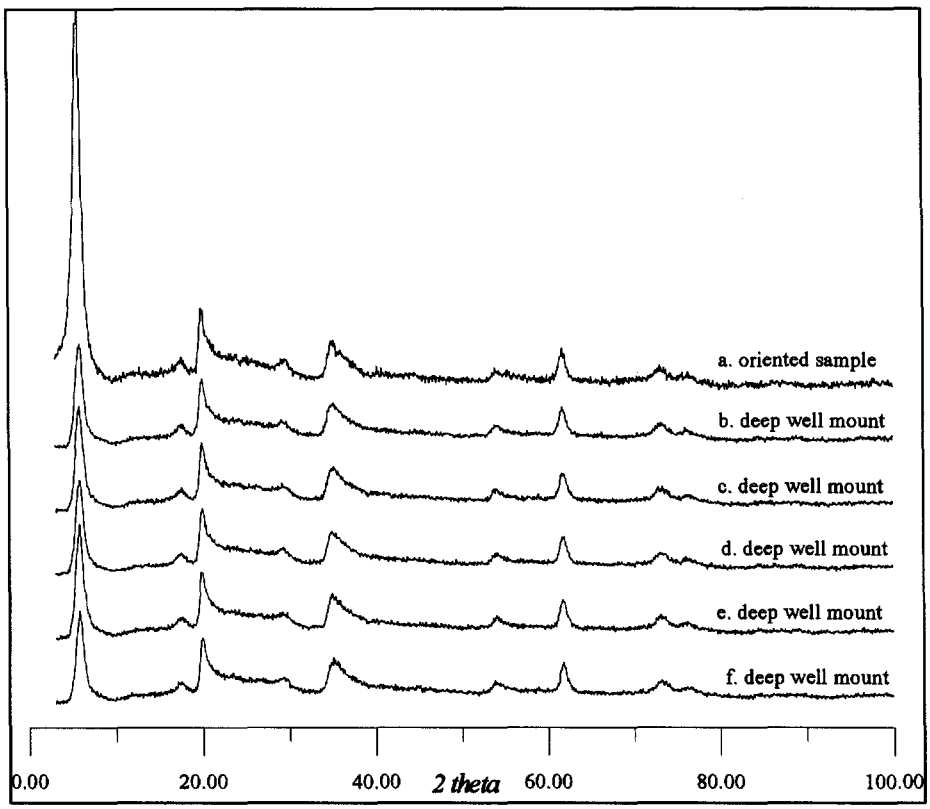

Figure 1. Diffraction patterns of montmorillonite (BM 32737) repacked 5 times in the same deep-well holder, b) to f); a) is the pattern produced by deliberately flattening the sample surface to induce preferred orientation.

tion, the pattern still portrays diffraction from the crystallite set closely representing random orientations. This method of sample preparation is highly reproducible and, coupled with the PSD geometry, is potentially of great value in constructing a future clay mineral database similar to that of Smith et al. 1995. Unlike scanning diffractometer systems with coupled θ-2θ geometry using a fixed θ incidence geometry, only 1 preferred orientation set (per phase), originating from sample flattening, is ever likely to be in Bragg orientation. This represents a very important difference between the stationary PSD and scanning methods and is one of the main reasons for the much improved quantification results reported here.

We do not claim to produce mounts with perfectly random orientation of particles; a degree of platelet orientation is present in our dry-packed mounts, as demonstrated by Figure 2. Decreasing the angle between the sample surface and the incident beam increases the 001 peak intensity as the Bragg angle is approached at low θ, illustrating the presence of some preferred orientation. Although the 001 peak at low 2θ shows considerable variation in intensity with beam incidence angle, the resulting difference in scattering at higher angles of 2θ is minimal. This characteristic of the PSD system allows patterns collected at different beam-incidence angles to be used in quantification because pattern matching is done at moderate to high 2θ, the 001 reflection being used only to aid initial clay mineral identification.

DATA ANALYSIS PROCEDURES

Sequential pattern-stripping (subtraction) was performed with ENRAF-GUFI software in order to identify and subtract each phase present in mixed-assemblage samples until the residual pattern indicated that no phases remained. This process provided a rapid quantitative assessment of the mineral phases present. Although the order in which the different minerals were removed did not affect the final quantification, generally the most easily identifiable phases, with sharp peaks, were stripped first, such as quartz and calcite. The remaining clay mineral phases were removed last as these have variable and broader peaks that required more careful matching to standards in order to minimize errors in quantification. For each phase identified, a single-phase standard pattern from the database, representing 100% of that phase, was superimposed upon the multiphase pattern. We then proportionally reduced the standard counts in order to achieve a best match (by eye) to that phase in the mul-

https://doi.org/10.1346/CCMN.1998.0460209 Published online by Cambridge University Press

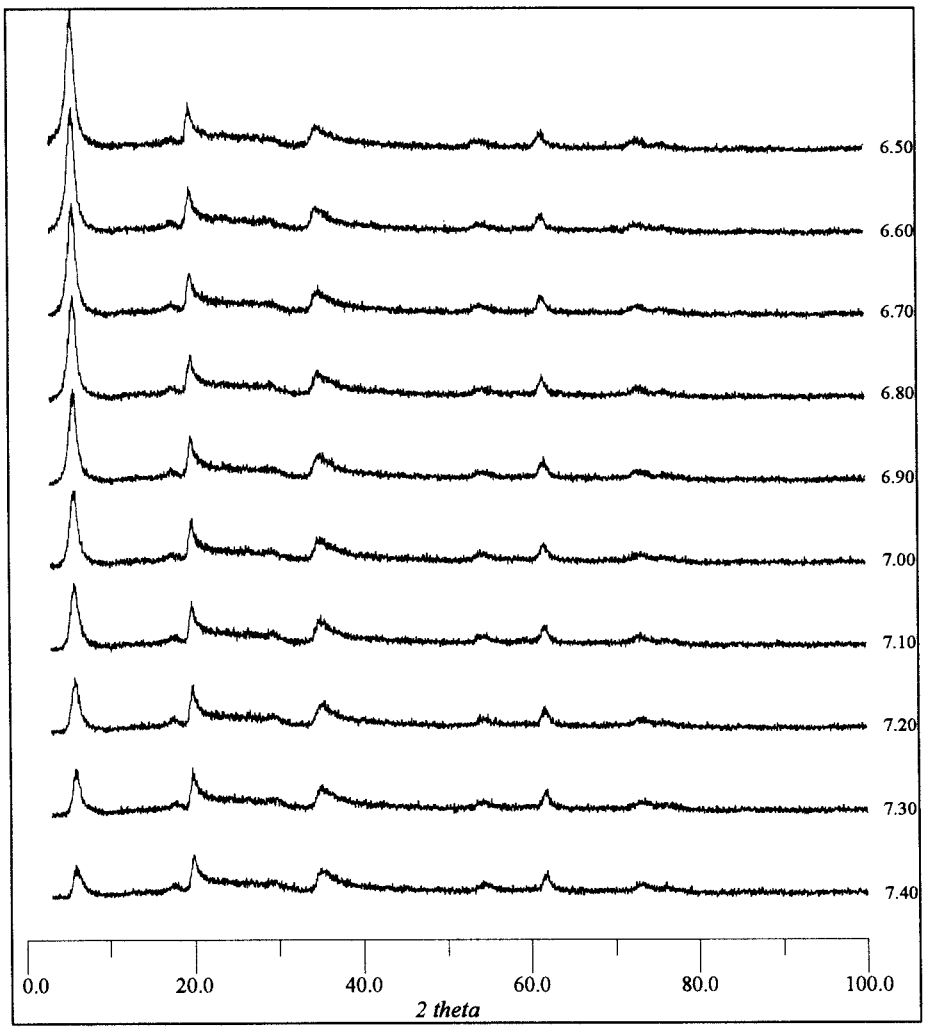

Figure 2. Effect on the diffraction pattern of montmorillonite (BM 32737) of increasing the angle of incidence between the beam and sample surface.

tiphase pattern. This process was rapid and only a few iterations were usually required to closely bracket the optimal fit. When a satisfactory fit was achieved, the scaling fraction was taken to represent the volume proportion in the sample. Subsequent stripping removed this component from the multiphase pattern and the procedure was repeated for the next phase, until the residual pattern showed that no phases remained. For mixtures containing a large number of components, it may be desirable to employ more sophisticated procedures for pattern analysis, such as simultaneous least-squares refinement (Smith et al. 1991).

The peak matching was done at moderate to high angles (40–110 °2θ) as preferred orientation is unlikely to occur at these angles and the errors produced by depth of penetration of the incident beam and changes in sample thickness are minimized. If no suitable standard is available or an unknown phase is present, stripping software can be used to remove all the known phases and the unmatched phase proportion assessed by difference. In practice we have found that the patterns of non-clay minerals (with well-defined peaks) can be fitted with a precision of ~1% fit of the standard pattern and those of clay minerals to within about 3% precision. Accuracy in determining phase proportions depends on the close matching with the standard pattern. Improvements in accuracy will be facilitated in the future by the compilation of a comprehensive database from well-characterized material. At low 2θ angles, discrepancies may occur from small degrees of preferred orientation of the clay minerals and enhanced reflections from single larger crystallites at the surface of the sample, but these minor differences can be ignored as they do not affect the quantification results.

Figure 3 is an example of a peak-stripping quantitative assessment of a binary clay mixture produced

https://doi.org/10.1346/CCMN.1998.0460209 Published online by Cambridge University Press

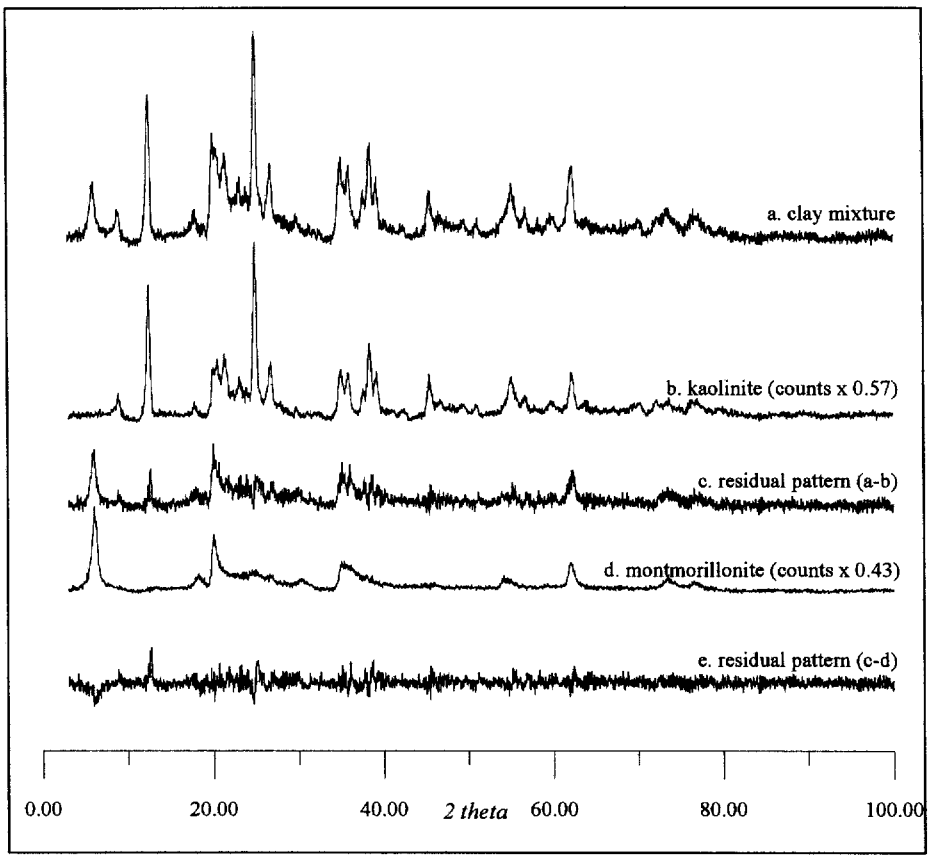

Figure 3. Whole-pattern matching and stripping of Mix 1 (kaolinite BM 1910,585 and montmorillonite BM 1986,472).

by combining kaolinite (containing a mica impurity) and montmorillonite in known amounts (Mix 1). The individual mineral patterns are shown reduced in intensity from unity by a fraction representing the measured volume proportion present. Residual patterns are shown with each phase stripped from the profile in turn. The known and measured proportions of the mixture are shown in Table 1. The phases in this mixture have very similar linear absorption coefficients (calculated from their chemical analyses and approximate densities) and consequently, as shown by the experimental result obtained, there is little need for an absorption correction factor to be applied in this case.

The peak-stripping steps for quantification were facilitated by comparison with diffraction patterns in our database of clay and non-clay minerals. Many clay-bearing samples commonly contain quartz, calcite, feldspar and iron oxide in addition to 1 or more clay minerals. Our growing database of digital whole-patterns not only provides important information on well-characterized minerals in the Museum collection but is invaluable as a reference tool for the identification and quantification of unknown samples. Reference clay minerals are often very difficult to obtain from the material to be analyzed (Brindley 1980). However, by building an extensive database, an appropriate match is more likely to be found that also takes into account variable degrees of disorder in clay structures (Smith et al. 1995).

Table 1. Calculated and measured mineral proportions of Mix 1 (kaolinite BM 1910,585 and montmorillonite BM 1986,472).

Mineral	Density (g cm^{-3})	μ (cm^{-1})	wt%	Actual volume %	Measured volume %
Kaolinite	~2.6	90	58	59	57
Montmorillonite	~2.7	100	42	41	43

CORRECTION FOR ABSORPTION

X-rays are attenuated by absorption as they pass through the sample. The mass absorption coefficient (μ/ρ) of the whole sample is simply a weighted average of the mass absorption coefficients of the constituent elements (Brindley 1980). The linear absorption coefficient (μ) is required for correction of intensity in Equation [3]; μ differs for each mineral in a mixture and is a function of the chemistry, density and wave-

https://doi.org/10.1346/CCMN.1998.0460209 Published online by Cambridge University Press

Table 2. Examples of μ for Cu radiation for several non-clay minerals commonly associated with sedimentary rocks.

Mineral	Formula	Density (g cm^{-3})	μ (cm^{-1})
Albite	$NaAlSi_3O_8$	2.62	90
Anorthite	$CaAl_2Si_2O_8$	2.76	145
Calcite	$CaCO_3$	2.71	202
Gypsum	$CaSO_4{\cdot}2H_2O$	2.32	149
Halite	NaCl	2.17	170
Hematite	Fe_2O_3	5.26	1140
Orthoclase	$KAlSi_3O_8$	2.57	123
Quartz	SiO_2	2.65	97

length of radiation used. Values of μ for each phase can be obtained by multiplying the computed mass absorption coefficient by the density of the mineral. If the minerals in a mixed assemblage sample have similar linear absorption coefficients then correction for absorption can, to a first approximation, be neglected (Cressey and Schofield 1996).

From our experimental work with mixtures of non-clay minerals in known proportions it is obvious that a correction factor must be applied to account for differences in the linear absorption coefficients of minerals that typically occur in sedimentary rocks. To demonstrate this, a binary quartz-calcite mixture of known volume ratio 1:1 was analyzed and the corresponding measured volume ratio was found to be 0.64:1.36, that is, the apparent proportion of calcite is significantly enhanced, an effect that is well known (Azároff and Buerger 1958). The disparity is a consequence of the difference in μ for quartz and calcite; μ^Q is 97 cm^{-1} and μ^C is 202 cm^{-1}; the ratio of μ^C/μ^Q is 2.08. Table 2 shows the variation in μ for several non-clay minerals commonly associated with clays in sedimentary rocks.

To determine the correction factors that must be applied in order to account for the effect of absorption, a series of binary mixtures containing different proportions of mineral phases with different μ values was analyzed. Four series of mixtures were weighed out: calcite and quartz ($\mu^C/\mu^Q = 2.08$); hematite and quartz ($\mu^H/\mu^Q \sim 11.75$); calcite and gypsum ($\mu^C/\mu^G \sim 1.36$) and gypsum and quartz ($\mu^G/\mu^Q \sim 1.54$). The actual volume ratios, measured volume ratios and absorption correction factors for the incremental calcite–quartz and hematite–quartz mixtures from 10% to 90% are given in Tables 3 and 4. From these results it is clear that the experimentally determined absorption correction factors are in excellent agreement with the theoretical values. Only in the extreme case of small amounts of a low absorber (quartz) in a highly absorbing matrix (hematite) does the absorption correction become slightly less reliable, because the errors in experimental assessment become large relative to the apparent amounts present.

Therefore correction for absorption can be calculated for a theoretical mixture of A and B, from their respective absorption coefficients μ^A and μ^B. Thus, an absorption correction diagram can be constructed and used to assess the correction factor required to convert measured volumes to actual volumes (Figure 4). To calculate the relationship between the measured volume and actual volume of phase A in a binary mixture of A and B, the linear absorption coefficient of the mixture (μ') is simply computed as:

$$\mu' = (x^A\mu^A) + (y^B\mu^B) \quad [4]$$

where x^A and y^B are the known volume fractions of phases A and B, respectively. The volume of phase A measured from the diffraction pattern will be given by:

$$v^A_{meas} = x^A\frac{\mu^A}{\mu'} \quad [5]$$

The experimental data presented in Tables 3 and 4 confirm Equation [5]. These experiments relating known to measured (apparent) volume fractions demonstrate that a correction factor for absorption can be made simply by applying a single scaling factor, μ'/μ^A; see Equation [5]. The apparent intensity of each

Table 3. Calculated and measured volume percentages of calcite and quartz mixtures where $\mu^C/\mu^Q = 2.08$. The final 2 columns of the table are the calculated absorption correction factors for a binary mixture series where $\mu^A/\mu^B = 2.08$ and are in excellent agreement with values of v^{known}/v^{meas} determined experimentally.

Mechanical mixture				Uncorrected values		Experimentally determined correction factors		Theoretical absorption correction factors	
wt% calcite	wt% quartz	Known vol% calcite	Known vol% quartz	Measured vol% calcite	Measured vol% quartz	v^k/v^m calcite	v^k/v^m quartz	$\frac{x\mu^A + y\mu^B}{\mu^A}$	$\frac{x\mu^A + y\mu^B}{\mu^B}$
90.20	9.80	90.0	10.0	95	5	0.95	2.00	0.95	1.97
80.36	19.64	80.0	20.0	89	11	0.90	1.82	0.90	1.87
70.47	29.53	70.0	30.0	83	17	0.84	1.76	0.84	1.76
60.54	39.46	60.0	40.0	76	24	0.79	1.67	0.79	1.65
50.56	49.44	50.0	50.0	68	32	0.74	1.56	0.74	1.54
40.54	59.46	40.0	60.0	58	42	0.69	1.43	0.69	1.43
30.47	69.53	30.0	70.0	47	53	0.64	1.32	0.64	1.32
20.36	79.64	20.0	80.0	34	66	0.59	1.21	0.58	1.22
10.20	89.80	10.0	90.0	19	81	0.53	1.11	0.53	1.11

https://doi.org/10.1346/CCMN.1998.0460209 Published online by Cambridge University Press

Table 4. Calculated and measured volume percentages of hematite and quartz mixtures where $\mu^H/\mu^Q = 11.75$. The final 2 columns of the table are the calculated absorption correction factors for a binary mixture series where $\mu^A/\mu^B = 11.75$ and are in excellent agreement with values of ν^{known}/ν^{meas} determined experimentally.

Mechanical mixture				Uncorrected values		Experimentally determined correction factors		Theoretical absorption correction factors	
wt% hemat.	wt% quartz	Known vol% hemat.	Known vol% quartz	Measured vol% hemat.	Measured vol% quartz	ν^k/ν^m hemat.	ν^k/ν^m quartz	$\frac{x\mu^A + y\mu^B}{\mu^A}$	$\frac{x\mu^A + y\mu^B}{\mu^B}$
94.70	5.30	90.0	10.0	99	1	0.91	~10	0.91	10.7
88.81	11.19	80.0	20.0	98	2	0.81	~10	0.82	9.60
82.24	17.76	70.0	30.0	97	3	0.72	~10	0.73	8.53
74.86	25.14	60.0	40.0	95	5	0.63	8.00	0.63	7.45
66.50	33.50	50.0	50.0	92	8	0.54	6.25	0.54	6.38
56.96	43.04	40.0	60.0	89	11	0.45	5.45	0.45	5.30
45.97	54.03	30.0	70.0	84	16	0.36	4.38	0.36	4.23
33.17	66.83	20.0	80.0	75	25	0.27	3.20	0.27	3.15
18.07	81.93	10.0	90.0	57	43	0.18	2.09	0.18	2.08

phase in the mixture is compared directly with the intensity pattern produced by the pure phase from an area of sample irradiated equal to the area of mixture irradiated. Thus, the scaling factor is a function of absorption, packing density and surface roughness (affecting beam penetration and volume irradiated).

Microabsorption (Wilchinsky 1951; Herman and Ermrich 1987) is a function of grain size and surface roughness of the sample irradiated, and can lead to an underestimate of the high-absorber phase in a mixture if its constituent grains are large (Bish and Reynolds 1989). However, using our method of sample preparation, we observe no evidence in our quantification results for the effects of microabsorption arising from different surface roughness of standard and mixture samples. If microabsorption is operative then we are able to achieve an equal degree of surface roughness and packing in the standard and sample experiments; with a spinning sample, surface roughness effects are averaged over a large area ($2\pi r^2 \approx 20$ mm^2) relative to the beam dimensions of 5×0.24 mm. In our experiments with binary hematite–quartz mixtures, each phase was ground only until smooth, then sieved to retrieve a <37 μm fraction before homogenizing the mixture. The majority of grains were observed optically to be in the range 5–20 μm for both hematite and quartz. Even using Cu radiation (absorption by hematite maximized), the effects of microabsorption did not affect the quantification. The results in Tables 3 and 4 demonstrate that reproducible surface roughness and packing density are easily achieved, and that apparent phase proportions can be regarded as being modified by matrix absorption effects alone.

For a mixture of A and B in unknown proportions, it is not possible to calculate the actual linear absorption coefficient of the matrix (μ') from Equation [4], because the volume fractions measured are not the true values. However, the true matrix absorption coefficient is related to an apparent matrix absorption coefficient (μ''), calculated from the measured (apparent) volume fractions, by a scaling factor of value s:

$$\mu' = s[(\nu^A_{meas}\mu^A) + (\nu^B_{meas}\mu^B)] \quad [6]$$

$$\mu' = s\mu'' \quad [7]$$

The value of $s\mu''$ may then be substituted in Equation [5] and by calculating phase proportions as ratios or as normalized quantities, the scale factor (value s) cancels out. Thus, the actual volume fraction x^A can be calculated simply from the measured volume fractions and linear absorption coefficients:

$$x^A = \frac{\nu^A_{meas}(\mu''/\mu^A)}{\nu^A_{meas}(\mu''/\mu^A) + \nu^B_{meas}(\mu''/\mu^B)} \quad [8]$$

Results calculated for the 2 test mixtures, calcite–quartz and hematite–quartz, using Equation [8] are shown in Table 5 and indicate that this correction procedure can be used with confidence, even in the case where the constituent phases of the mixture have very different absorption coefficients.

This approach can be extended to any multiphase system and in the general case with i phases:

$$\mu' = \sum_i x_i\mu_i \quad [9]$$

and,

$$\mu'' = \sum_i \nu_i\mu_i \quad [10]$$

with

$$\mu' = s\mu''$$

where x_i is the actual volume fraction, ν_i is the measured (apparent) volume fraction, μ_i is the linear absorption coefficient of phase i and s is a scale factor. These values can be substituted in Equation [5] and proportions normalized to give actual volume fractions:

https://doi.org/10.1346/CCMN.1998.0460209 Published online by Cambridge University Press

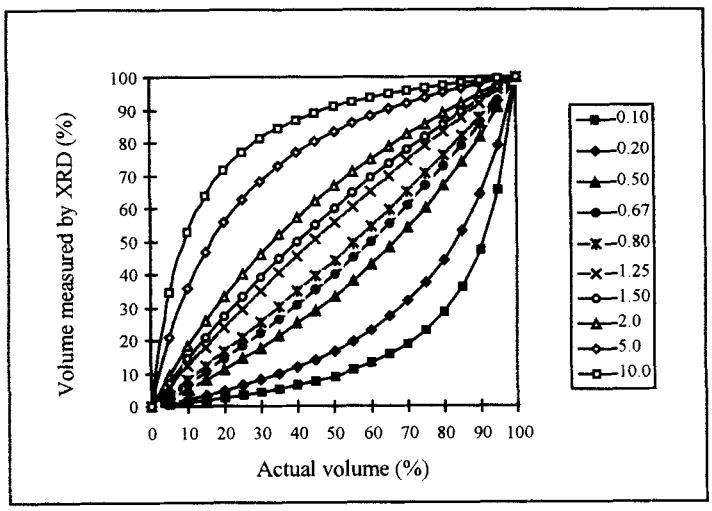

Figure 4. Absorption correction factors shown for 5 binary series with different μ ratios, calculated from theoretical μ values.

$$x_i = \frac{v_i(\mu''/\mu_i)}{\sum_i v_i(\mu''/\mu_i)} \qquad [11]$$

The speed and reliability of this quantification technique and the efficacy of the absorption correction have been tested by quantitatively analyzing a ternary mixture of clay minerals. This mechanical mixture (Mix 2) was chosen specifically to assess possible problems arising from variations in density, grain size and iron content. Mix 2 contains kaolinite, montmorillonite and an illite (BM 1910,585; BM 32737 and BM 1951,323 respectively) and the whole-pattern matching and stripping is shown in Figure 5. Numerical results and the correction for absorption using Equation [11] are shown in Table 6 and demonstrate that these adjustments are of the correct magnitude; excellent agreement between the known and assessed proportions has been achieved. Furthermore, this total analysis was performed in only a few minutes.

In applying corrections for absorption in mixtures involving clay minerals, it is assumed that the linear absorption coefficient of the clay mineral is equal to that of the characterized clay mineral standard to which it is matched. The assumption is reasonable if the patterns match in all other respects. Differences in absorption coefficients of clay mineral species are predominantly controlled by the iron content of the clay. It is interesting to note that in matching patterns against standard clays we have found that the Fe content can also be rapidly assessed by matching the level of Fe X-ray fluorescence (XRF) that contributes to the background when using Cu radiation. The undulations present in the background patterns of Fe-bearing samples result from the way in which the detector responds when flooded with fluorescence radiation (as parasitic radiation at all angles) in addition to Cu wavelength radiation at the same time. Although not fully understood, it is thought that these undulations are a function of interference between pulses caused by the presence of different wavelengths in the detector. This effect is common to all PSD detectors of this type; the intensity, shape and position of undulations

Table 5. Comparison of known and absorption-corrected volume proportions in test mixtures of calcite–quartz and hematite–quartz. Absorption corrections using Equation [8] assume no knowledge of actual volumes and are based solely on measured (apparent) volumes. See Tables 3 and 4 for measured volume proportions.

Mechanical mixture		A : B mixture calcite–quartz		A : B mixture hematite–quartz	
Known vol% A	Known vol% B	Corrected meas. vol% calcite	Corrected meas. vol% quartz	Corrected meas. vol% hematite	Corrected meas. vol% quartz
90	10	90.1	9.9	89.4	10.6
80	20	79.5	20.5	80.6	19.3
70	30	70.1	29.9	73.3	26.7
60	40	60.3	39.7	61.7	38.2
50	50	50.5	49.5	49.5	50.5
40	60	39.9	60.1	40.8	59.2
30	70	29.9	70.1	30.9	69.1
20	80	19.8	80.2	20.3	79.7
10	90	10.1	89.9	10.1	89.9

https://doi.org/10.1346/CCMN.1998.0460209 Published online by Cambridge University Press

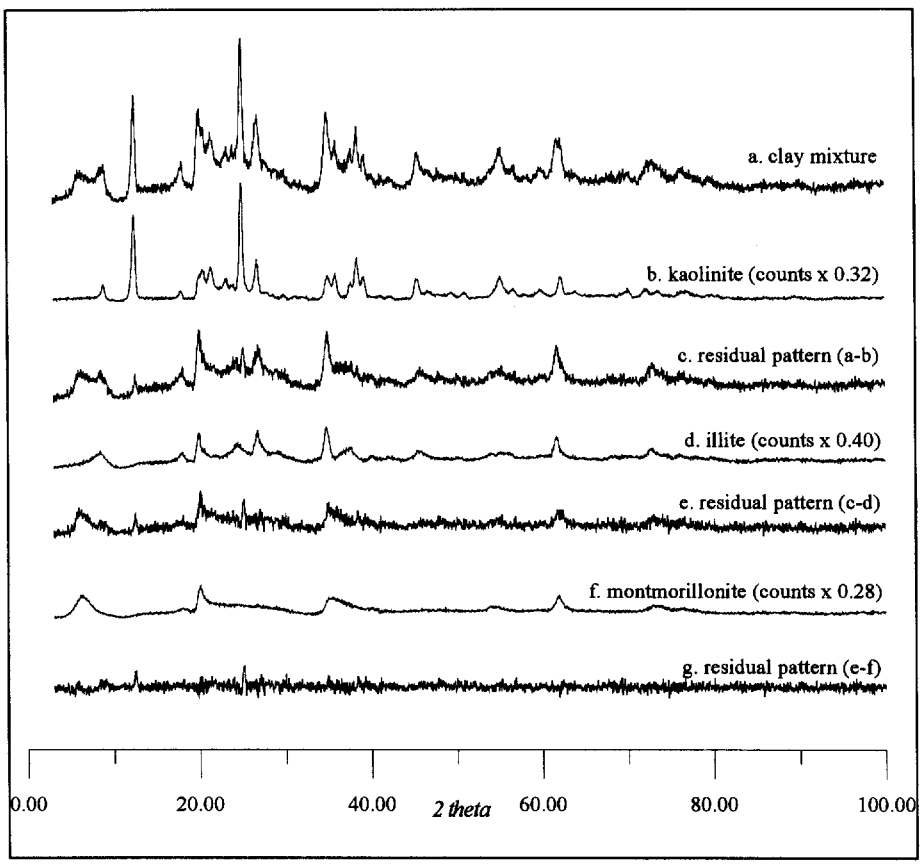

Figure 5. Whole-pattern matching and stripping of Mix 2 (kaolinite BM 1910,585: illite BM 1951,323 and montmorillonite BM 32737).

vary for each detector, but are stable with time for any particular detector. Because this undulatory background XRF signature is characteristic and reproducible for all Fe-phase patterns, this signal can be used to obtain rapid semiquantitative information on total Fe levels by deliberately using Cu rather than Co radiation. Clay minerals are matched to those in the database by degree of ordering, peak intensity and background (fluorescence) levels. Table 7 shows 5 groups represented in our clay mineral database. The groups, based on mineral chemistry, illustrate the effect of Fe-content on absorption coefficients.

Table 6. Calculated and measured mineral proportions of Mix 2 (kaolinite BM 1910,585, illite BM 1951,323 and montmorillonite BM 32737).

Mineral	Density (g cm^{-3})	μ (cm^{-1})	wt%	Actual volume %	Measured volume %	Corrected volume %
Kaolinite	2.63	91	35.2	37.0	32	37
Montmorillonite	~2.7	105	29.9	27.2	28	28
Illite	~2.7	120	34.9	35.8	40	35

Quantification using known mixtures is relatively uncomplicated as minerals can be matched exactly. Clay mineral identification and quantification for industrial applications and environmental purposes often employ clay mineral standards that are not identical to the phases in the sample. To test the efficiency of our method and its ease of use, the same quantification method was used to analyze a specimen of the Ruabon Marl collected from Gardden Lodge, near Ruabon, North Wales (NGR SJ330435). The sample was gently ground and then sieved to <37 μm. The powder was investigated optically and the predominant size of the particles was between 5–20 μm; a range matching that of our pure standards, so microabsorption effects are likely to cancel out, as we have observed for our hematite–quartz quantification experiments. The sample of Ruabon Marl contains 4 phases: hematite, quartz, kaolinite and illite. The phase proportions were assessed by whole-pattern matching and stripping in the usual way (Figure 6). The clay mineral standards selected from the PSD database were chosen for similarities in diffraction peak width and peak intensities. Residual peaks can also sometimes result from a slight

https://doi.org/10.1346/CCMN.1998.0460209 Published online by Cambridge University Press

Table 7. Groups of clay minerals used for quantification demonstrating the small standard deviation in linear absorption coefficient for each of the groups.

	Kaolinite	Low-Fe illites	High-Fe illites	Low-Fe montmorillonites	High-Fe montmorillonites
No. samples analyzed	12	12	6	14	6
Average μ/ρ	32.7	42.5	52.5	36.4	45.0
Limit of μ/ρ	all	<45	>45	<45	>45
Range of densities	2.60	2.60–2.80	2.60–2.80	2.50–2.90	2.50–2.90
Average μ	86.5	117.3	147.2	98.3	121.4
Standard deviation	0	3.4	3.9	5.8	7.1

2θ shift between the standard and sample patterns. These mismatches can be explained by imperfect transferability of the 2θ linearization function between samples via the external silicon standard, probably arising from inexact sample height reproducibility. Hematite has an absorption coefficient approximately 12 times that of the other 3 phases, resulting in an enhanced measured volume for hematite with respect to quartz, kaolinite and illite. Correction for absorption was achieved using Equation [11] and the results are presented in Table 8.

Chemical analysis by HF digestion and ICP/AES of this sample of Ruabon Marl was performed and the Fe_2O_3 content determined to be 6.15 wt%. Recalculating as volume percent gives a value of 3.1% Fe_2O_3, in excellent agreement with the XRD quantification of 3.6% hematite. For naturally occurring, mixed-assemblage samples a simple chemical analysis can provide

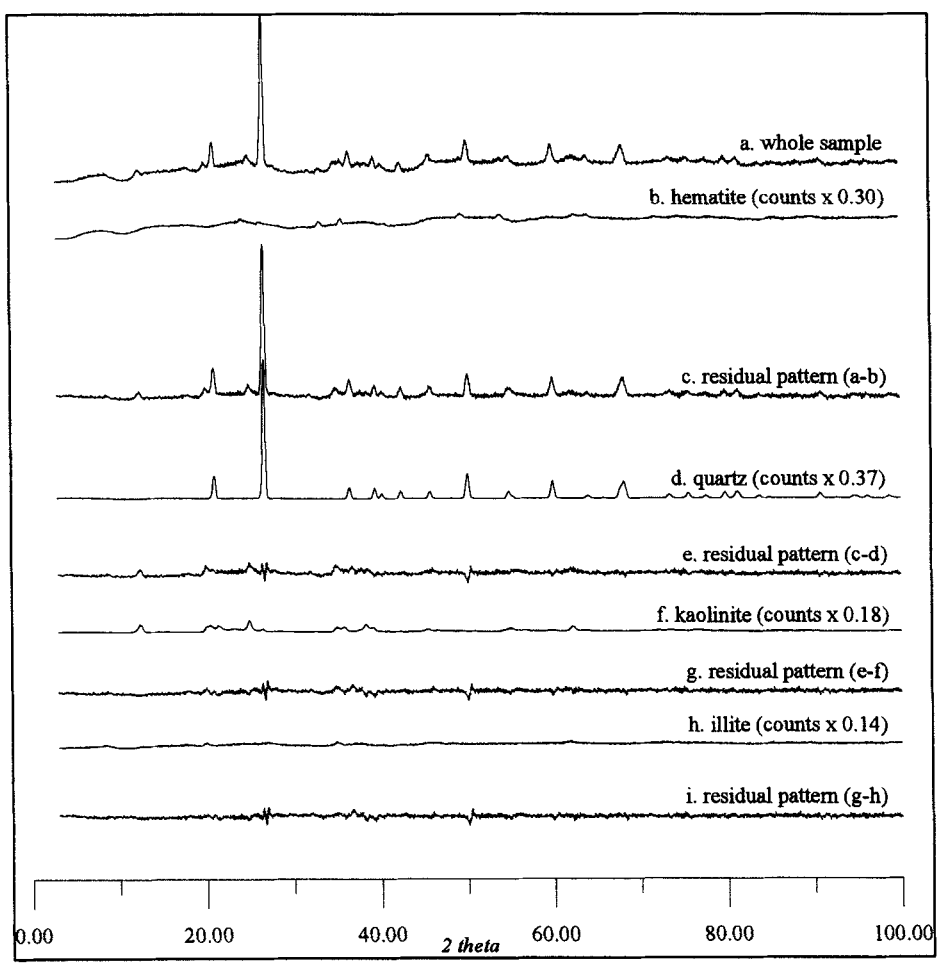

Figure 6. Whole-pattern matching and stripping of Ruabon Marl.

https://doi.org/10.1346/CCMN.1998.0460209 Published online by Cambridge University Press

Table 8. Measured and absorption-corrected mineral proportions determined for the Ruabon Marl.

Mineral	Density (g cm^{-3})	μ (cm^{-1})	Measured volume %	Corrected volume %
Hematite	5.26	1140	30	3.6
Quartz	2.65	97	37	52.7
Kaolinite	~2.6	~90	18	27.6
Illite	~2.7	~120	14	16.1

useful corroborative information in confirmation of quantitative estimates. The absorption coefficient of a sample can also be dramatically affected by the presence of small quantities of accessory minerals (easily identifiable by analytical SEM), so simple chemical analyses are always desirable.

CONCLUSIONS

In comparison with other methods of quantitative analysis, such as the use of internal standards or Rietveld methods, the technique described here is exceedingly rapid and involves only simple data processing. We have demonstrated that this method overcomes many of the inherent problems associated with quantification. The results obtained from the analysis of known mixtures confirms that the technique can be applied with confidence to quantify natural mudrocks. This alternative method has direct relevance to problem solving associated with the use of clays in environmental waste management, the petroleum industry and many other industrial applications.

The PSD quantification procedure involves pattern matching and pattern stripping using methods that are well established for handling digital data. However, one area in which our method is superior over that of Smith et al. (1987) is that it requires no calibration by spiking with reference intensity ratio (RIR) materials. The detector stability and pattern reproducibility are excellent when using the stationary geometry of a PSD system for which pattern intensity is simply a function of acquisition time and total X-ray flux. Therefore, whole patterns can be compared directly and rapidly with an existing whole-pattern database. We can precisely reproduce patterns from the same sample in experiments performed over 1 year apart, because any differences in total flux can be easily assessed and adjusted for using an (external) silicon standard. This means that in the future, patterns and their intensities acquired in different laboratories can be intensity calibrated, enabling the direct comparison of patterns for quantification purposes. The speed of our method is also unique; pattern acquisition times of only a few minutes are sufficient for accurate assessment of phase proportions. Our method also allows corrections for absorption to be applied quickly in a straightforward manner from first principles, provided that the phases in the mixture are identified and particle sizes of standards and mixtures are comparable. Taken collectively, these factors result in a robust new method for phase quantification. In many respects, the PSD system is able to provide a better approach to clay mineral studies, because highly reproducible whole-pattern data from near-randomly oriented samples can be acquired easily and rapidly. In addition, for the difficult task of quantifying phase proportions in clays and mudrocks, the PSD approach is proving to be particularly beneficial.

ACKNOWLEDGMENTS

The authors wish to extend many thanks to Shanks and McEwan Ltd., especially J. B. Joseph, for providing both financial support and materials.

REFERENCES

Azároff LV, Buerger MJ. 1958. The powder method. New York: McGraw-Hill. 342 p.

Bish DL, Howard SA. 1988. Quantitative phase analysis using the Rietveld method. J Appl Crystallogr 21:86–91.

Bish DL, Reynolds RC Jr. 1989. Sample preparation for X-ray diffraction. In: Bish DL, Post JE, editors. Modern powder diffraction. Washington, DC: Rev Mineral 20. Mineral Soc Am. p 73–97.

Brindley GW. 1980. Quantitative X-ray mineral analysis of clays. In: Brindley GW, Brown G, editors. Crystal structures of clay minerals and their X-ray identification. London: Mineral Soc. p 411–438.

Chung FH. 1974a. Quantitative interpretation of X-ray diffraction patterns of mixtures. I. Matrix flushing method for quantitative multicomponent analysis. J Appl Crystallogr 7:519–525.

Chung FH. 1974b. Quantitative interpretation of X-ray diffraction patterns of mixtures. II. Adiabatic principle of X-ray diffraction analysis of mixtures. J Appl Crystallogr 7: 526–531.

Cressey G, Schofield PF. 1996. Rapid whole pattern profile-stripping method for the quantification of multiphase samples. Powder Diff 11:35–39.

Foster BA, Wolfel ER. 1988. Automated, quantitative multiphase analysis using a focussing transmission diffractometer in conjunction with a curved position-sensitive detector. Adv X-Ray Anal 31:325–330.

Herman H, Ermrich M. 1987. Microabsorption of X-ray intensity in randomly packed powder specimens. Acta Crystallogr A43:401–405.

Hill RJ, Howard CJ. 1987. Quantitative phase analysis from neutron powder diffraction using the Rietveld method. J Appl Crystallogr 20:467–474.

McManus DA. 1991. Suggestions for authors whose manuscripts include quantitative clay mineral analysis by X-ray diffraction. Marine Geol 98:1–5.

Moore DM, Reynolds RC Jr. 1989. X-ray diffraction and the identification and analysis of clay minerals. Oxford: Oxford Univ Pr. 332 p.

Smith DK, Johnson GG Jr, Hoyle SQ. 1991. MATCHDB—A program for the identification of phases using a digitized diffraction-pattern database. Adv X-Ray Anal 34:377–385.

Smith DK, Johnson GG Jr, Jenkins R. 1995. A full-trace database for the analysis of clay minerals. Adv X-Ray Anal 38:117–125.

Smith DK, Johnson GG Jr, Scheible A, Wims AM, Johnson JL, Ullmann G. 1987. Quantitative X-ray powder diffrac-

tion method using the full diffraction pattern. Powder Diff 2:73–77.
Snyder RL, Bish DL. 1989. Quantitative analysis. In: Bish DL, Post JE, editors. Modern powder diffraction. Washington, DC: Rev Mineral 20. Mineral Soc Am. p 101–142.
Wilchinsky ZW. 1951. Effect of crystal, grain, and particle size on X-ray power diffracted from powders. Acta Crystallogr 4:1–9.

(Received 13 May 1996; accepted 1 July 1997; Ms. 2765)